

C80-058

# Development of a Helicopter Rotor Hub Elastomeric Bearing

00013  
00026  
00031

P. Donguy\*

Société Européenne de Propulsion, Saint-Médard-en-Jalles, France

The theme of this paper is to present recent advances in the field of elastomeric bearings for light helicopter rotor hubs. These bearings are spherical hinges able to withstand centrifugal and lateral forces during torsional, flap, and lead-lag motions. Service life has been the principal problem encountered during their development. Test results were obtained from different types of bearings and the analyses of these data resulted in the hydroflex bearing. This bearing encloses a liquid in the bearing and significantly increases service life. This paper presents a review of the analyses of the test data and describes the hydroflex bearing.

## Introduction

THE articulated rotor hub of a helicopter traditionally is a complex device. Each rotor blade is usually linked to the hub by three hinges allowing pitch, lead-lag, and flap motions. These hinges generally are made with roller and ball bearings and require lubrication. The bearings transmit high loads and operate in adverse conditions due to the oscillating motions of the blades. To simplify the helicopter rotor hub and reduce maintenance, the trend now is to replace the roller and ball bearings by elastomeric bearings consisting of alternate thin laminations of elastomer and metal bonded together. This paper reviews the development of such a bearing that withstands all required loads and demonstrates a satisfactory service life.

## Why Elastomeric Bearings?

Laminations of elastomer and metal are particularly suited to the requirements of rotor hub bearings, able to withstand high, axial loads along the bearing while allowing oscillating motions. Furthermore, several kinds of oscillating motions can be combined in one elastomer bearing by suitably shaping the laminations. The sphere is of most particular interest since it allows oscillation about three perpendicular axes (see Fig. 1). The spherical bearing is the topic of this paper. Such a bearing needs no lubrication and replaces three conventional bearings resulting in a simplification and reduction in the number of components of the rotor hub.

## Spherical Elastomeric Bearings Requirements

The following requirements were taken into account for the definition of the spherical elastomeric bearings.

### Maximum Displacements

Pitch angle:  $\pm 20$  deg  
Flap angle:  $\pm 8$  deg  
Lead-lag angle:  $\pm 1$  deg

### Maximum Loads

Along  $Oy$  axis: Compressive load: 137,000 N  
Ultimate compressive load: 165,000 N  
Along  $Ox$  axis:  $F_x = 5000$  N.

Presented as Paper 79-0815 at the AIAA/ASME/ASCE/AHS 20th Structures, Structural Dynamics & Materials Conference, St. Louis, Mo., April 4-6, 1979; submitted May 21, 1979; revision received Dec. 17, 1979. Copyright © American Institute of Aeronautics and Astronautics, Inc., 1979. All rights reserved. Reprints of this article may be ordered from AIAA Special Publications, 1290 Avenue of the Americas, New York, N.Y. 10019. Order by Article No. at top of page. Member price \$2.00 each, nonmember, \$3.00 each. **Remittance must accompany order.**

Index categories: Helicopters; Propeller and Rotor Systems; Subsystem Design.

\*Manager Advanced Products.

### Stiffness

Compressive stiffness along  $Oy$  axis: approximately 100,000 N/m

Lateral stiffness along  $Ox$  or  $Oz$  axis: greater than 10,000 N/m

Torsional stiffness about  $Oy$  axis: less than 4 m. N/deg

Torsional stiffness about  $Ox$  or  $Oz$  axis: approximately 10 m. N/deg

### Operational Temperature Range

The required operational temperature range is  $-54$  to  $+54^\circ\text{C}$ . With zero motion and load (helicopter grounded), the required range is  $-54$  to  $+90^\circ\text{C}$ .

### Service Life

The required service life is 2000 h with the following mean loads and motions ( $t$  is the time in seconds):

Compressive load along  $Oy$  axis: 137,000 N

Load along  $Ox$  axis:  $(3000 + 2000 \sin 12\pi t)$  N

Torsional motion about  $Oy$  axis:  $(5 + 5.7 \sin 12\pi t)$  deg

Torsional motion about  $Ox$  axis:  $(3.5 \sin 12\pi t)$  deg.

## Preliminary Bearing

### Factors Affecting Service Life

To design and dimension this preliminary flexible bearing, it was necessary to define the factors affecting service life. Tests were conducted on samples of natural rubber applying various loads and motions. The results were as follows.

The service life of the rubber is primarily dependent upon the oscillating shear stress due to the oscillating motions or oscillating loads combined with a constant shear stress due to a compressive load and a constant distortion. For all regions in the lamination, the service life of the rubber may be written as

$$T = \frac{C}{\tau_D^{2.6} (1 + \tau_s)^{2.3}} \quad (1)$$

where  $\tau_s$  is the shear stress due to a constant compressive load and a constant distortion;  $\tau_D$  is the maximum shear stress due to an oscillating motion or an oscillating compressive load; and  $C$  is the parameter depending upon the shape of the flexible bearing and the rubber.

The service life of the flexible bearing is calculated in the most highly stressed region of the rubber in terms of service life. This service life is defined as the time when a component would normally be removed from service.

In Eq. (1), the shear stress  $\tau_s$  accounts for the constant compressive loads along the  $Oy$  (137,000 N) and  $Ox$  axes (3000 N) and the constant pitch angle (5 deg), while the shear stress  $\tau_D$  accounts for the oscillating motions in pitch and flap about the  $Ox$  and  $Oy$  axes ( $3.5 \sin 12\pi t$ ) deg and ( $5.7 \sin 12\pi t$ ) deg.

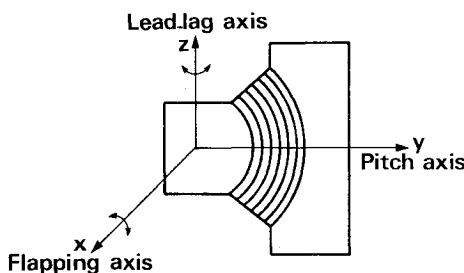


Fig. 1 Spherical bearing.

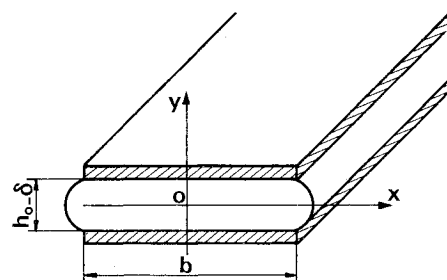


Fig. 3 Crushed elastomer layer.

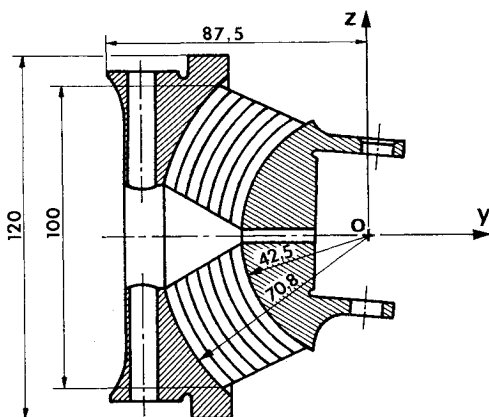


Fig. 2 Preliminary bearing.

deg and the oscillating compression load along the  $Ox$  axis  $(2000 \sin 12\pi t)$  N.

#### Design of the Preliminary Flexible Bearing

The requirements for this bearing were in part contradictory. A long service life requires a reduction of the dynamic shear stress due to oscillating torsional motions about the  $Oy$  axis through an increase of the total thickness of the rubber layers. Such an increase reduces the torque about the  $Oy$  axis, but also reduces the lateral stiffness along the  $Ox$  and  $Oz$  axes. Similarly, a low torsional torque and a high compressive stiffness along the  $Oy$  axis is contradictory.

The design of this preliminary, flexible spherical bearing was a compromise, having been designed with a compact shape and a laminate consisting of thin layers of rubber in order to meet the stiffness requirements along the  $Ox$  and  $Oy$  axes, and with a low shear modulus rubber selected to reduce the torsional torque about the  $Oy$  axis. The design of this bearing is shown in Fig. 2.

The lamination consists of 16 spherical concentric stainless steel shims as the attachments. The shims are 0.8 mm thick. The thickness of the rubber layers increases as the spherical radius increases from 0.7 to 1.1 mm.

The thicknesses of the rubber layers and the shims have been selected taking into account the manufacturing process, transfer molding of the rubber, and the behavior of the shims during the molding process.

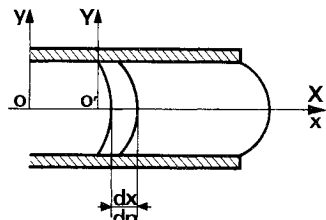
The selected elastomer is a natural rubber whose shear modulus is 0.29 MPa (rubber A). This rubber is particularly suitable because of its high mechanical strength and behavior at low temperature.

#### Test Results of Preliminary Flexible Bearing

The bearing withstood the loads and transmitted the motions required with no observed problems as a function of the temperature. The measured stiffnesses are: compressive along the  $Oy$  axis is 115,000 N/mm, and torsional about the  $Oy$  axis is 2 m·N/deg.

This bearing has been flight tested on a prototype helicopter, but its service life was only 500 h.

Fig. 4 Elastomer distortion under compression.



#### Flexible Bearing with a Modified Elastomer

A new blend of elastomer was selected after laboratory fatigue tests. This elastomer (rubber B) is primarily a natural rubber formulation with a slightly increased shear modulus 0.49 MPa. With this rubber the service life of the flexible bearing increased from 500 to 1500 h.

Because of the change of the shear modulus, the new stiffnesses of the bearing were: compressive along the  $Oy$  axis 167,000 N/m, and torsional about the  $Oy$  axis 3.8 m·N/deg.

These stiffnesses fulfill the requirements, but while the increased service life was significant, it was not sufficient and a new optimized bearing was studied.

#### Optimized Bearing

The region where the fatigue process commenced was at the inner diameter of the rubber layer located at the smallest spherical radius. The aim of a new optimized design of the bearing was to reduce the combined stresses in this region.

#### Shaping Method

The first step was to determine the stresses in the layers of elastomer due to a compressive load along the  $Oy$  axis and a torsional motion about the  $Ox$  and  $Oy$  axes.

The following method was used for the analysis of the stresses due to compressive loads along the  $Oy$  axis. The shear modulus  $G$  of the elastomer is assumed to be constant with respect to strain. The metal shims are assumed to be rigid. The basis of the analysis is that the elastomer is in an intermediate state between solid and liquid (Poisson ratio near 0.5). When a layer of elastomer is crushed, pressures appear in the elastomer (as a liquid) and these pressures are retained by shear stresses (as a solid). The analysis will be described for an infinite length strip of elastomer bonded to two rigid metallic shims. The analysis for spherical layers is conducted in the same manner, but the equations are complex and are numerically solved using a computer.

The infinite length strip bonded to two metallic shims has a width  $b$  and a thickness  $h_0$  before being compression loaded and  $(h_0 - \delta)$  after being loaded (Fig. 3).

The distorted surface  $Y(X)$  in  $O'$  (Fig. 4) when a change of pressure occurs for a displacement  $dx$  is given by:

$$Ydp = G \frac{dX}{dY} dx \quad (2)$$

or

$$dX = \frac{dp}{dx} \frac{1}{G} YdY$$

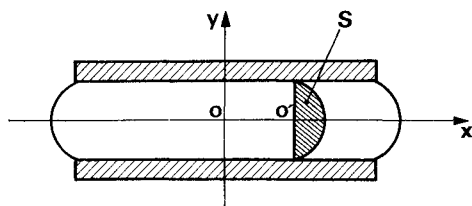


Fig. 5 Elastomer displacement under compression.

$$X = \frac{dp}{dx} \frac{1}{G} \left( \frac{Y^2}{2} + \text{constant} \right)$$

for  $X=0$ ,

$$Y = (h_0 - \delta)/2$$

$$X = \frac{dp}{dx} \frac{Y^2 - [(h_0 - \delta)^2/4]}{2G} \quad (3)$$

The distorted surface  $Y(X)$  is then a parabola (Fig. 5). The amount of elastomer displaced  $S$  beyond  $O'$  by unit of length is given by:

$$S = 2 \int_0^{(h_0 - \delta)/2} X dY$$

$$S = -\frac{1}{12} \frac{(h_0 - \delta)^3}{G} \frac{dp}{dx}$$

Between  $O$  and  $x$ , the volume of elastomer-displaced  $V_1$ , beyond  $x$  by unit of length is given by:

$$V_1 = -\frac{1}{12} \frac{(h_0 - \delta)^3}{G} \frac{dp}{dx}$$

The loss of elastomer due to the compressibility of the elastomer between  $O$  and  $x$  can be deduced from the equation:

$$\Delta V/V = -p/K$$

where  $K$  is the bulk factor

$$d(\Delta V) = (h_0 - \delta) \frac{p}{K} dx$$

$$\Delta V = \frac{h_0 - \delta}{K} \int_0^x pdx$$

The change of volume  $V_2$  of the elastomer between  $O$  and  $x$  due to the crushing is given by:

$$V_2 = \delta x$$

and

$$V_2 = \Delta V + V_1$$

$$\delta x = \frac{h_0 - \delta}{K} \int_0^x pdx - \frac{1}{12} \frac{(h_0 - \delta)^3}{G} \frac{dp}{dx}$$

$$-\frac{d^2p}{dx^2} + W^2 p = W^2 \frac{K}{h_0 - \delta}$$

where

$$W^2 = \frac{12G}{(h_0 - \delta)^2 K}$$

$$p = C_1 e^{wx} + C_2 e^{-wx} + \frac{\delta K}{h_0 - \delta}$$

If the external pressure is  $P_e$ , the boundary conditions are:

$$x = b/2 \quad p = P_e$$

$$v = -b/2 \quad p = P_e$$

These boundary conditions determine the constants  $C_1$  and  $C_2$ .

$$p = \frac{P_e - (\delta K/h_0 - \delta)}{e^{wb/2} + e^{-wb/2}} (e^{wx} + e^{-wx}) + \frac{\delta K}{h_0 - \delta}$$

It is also possible to determine  $C_1$  and  $C_2$  for two different external pressures, but it is necessary to locate the  $O$  point where the derivative of the pressure  $dp/dx$  is zero.

This evolution of pressure is linked to the compression force per unit of length  $F$  where:

$$F = - \int_{-b/2}^{b/2} pdv$$

Hence the crushing  $\delta$  is related to the force  $F$  by the equation:

$$F = -\frac{2}{w} \left( P_e - \frac{\delta K}{h_0 - \delta} \right) \tanh(wb/2) - \frac{\delta K}{h_0 - \delta} b$$

The definition of the stresses in the elastomer is obtained from the determination of the pressure by means of Eq. (2). The highest shear stresses  $\tau_c$  occur at the bonded interface of the elastomer to the metallic shims and are given by:

$$(h_0 - \delta) dp = 2\tau_c dx$$

$$\tau_c = \frac{h_0 - \delta}{2} \frac{dp}{dx}$$

$$\tau_c = -w \left( \frac{h_0 - \delta}{2} \right) \left( P_e - \frac{\delta K}{h_0 - \delta} \right) \frac{\sinh w_x}{\cosh w b/2}$$

The stresses are a maximum at the edges of the shims,  $x = \pm b/2$ .

Stresses induced by torsional motions about the  $Ox$  or  $Oy$  axes, the shear modulus  $G$  of the elastomer is also assumed to be constant as a function of strain. For all points in the elastomer layer, the shear stresses  $\tau$  are linked to the shear strain  $\gamma$  by the equation:

$$\tau = G\gamma$$

The torsional stiffness of all layers are calculated and, since the spring torques due to torsional motions of all layers are equal, it is possible to calculate the stresses and strains in each layer due to a torsional motion about the  $Ox$  or  $Oy$  axes.

#### Stress Analysis of the Rubber of the Preliminary Flexible Bearing

This analysis has been conducted using rubber B. The following results were obtained for the most severe combination of stresses in terms of service life (see Fig. 6). The pressure distribution  $P$  in the rubber layer is due to a 137,000 N compressive force along the  $Oy$  axis; the stresses  $\tau_s$  were due to a 5 deg torsional motion about the  $Oy$  axis; the stresses  $\tau_D$  were due to a 5.7 deg torsional motion along the  $Oy$  axis and a 3.5 deg torsional motion about the  $Ox$  axis. Pressure and stresses are expressed in bar (Fig. 7).

The lateral force along the  $Ox$  axis has been neglected because this force is small.

#### Design of the Optimized Flexible Bearing

The thicknesses of the layers of rubber situated at the largest spherical radius have been increased to reduce the oscillating shear stresses in the layers of rubber situated at the

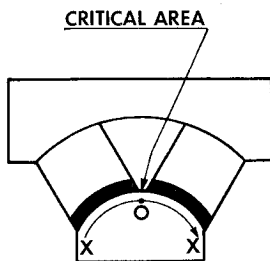


Fig. 6 Preliminary bearing—critical area.

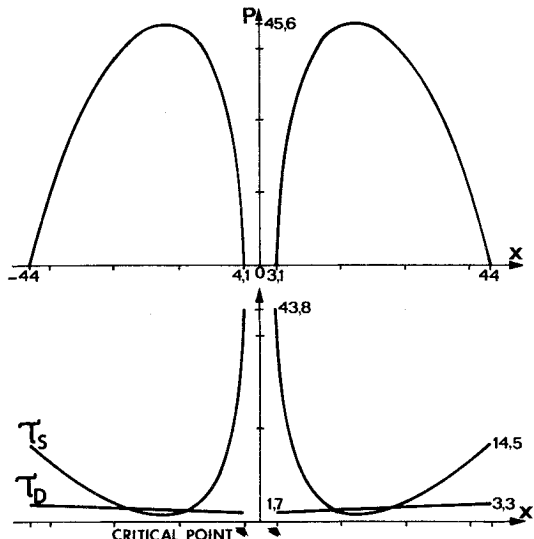


Fig. 7 Preliminary bearing—pressure and stress distributions.

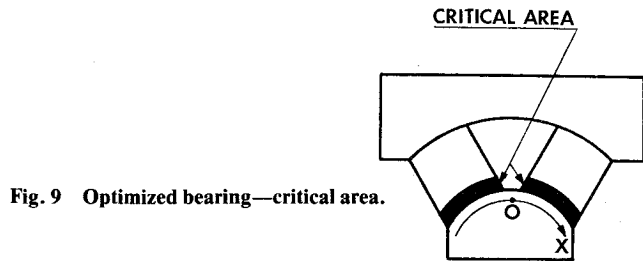


Fig. 9 Optimized bearing—critical area.

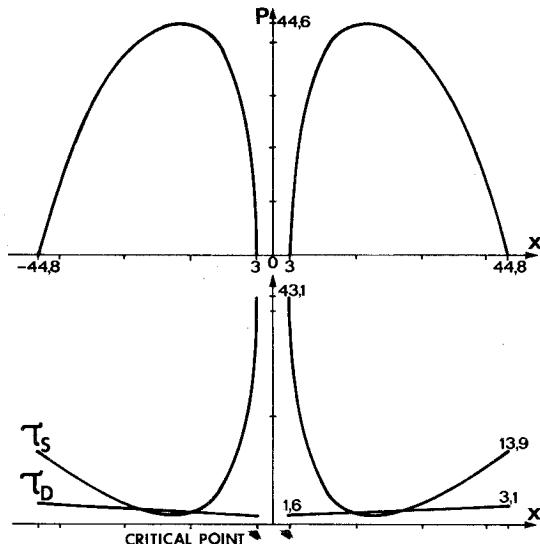


Fig. 10 Optimized bearing—pressure and stress distribution.

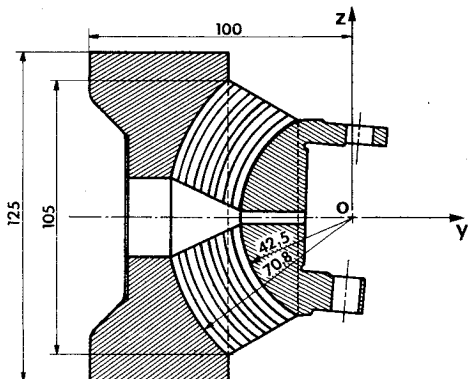


Fig. 8 Optimized flexible bearing.

smallest spherical radius. Also, the area of the layers at the largest spherical radius has been increased slightly. The new design of the bearing is shown in Fig. 8.

The attachments are aluminum alloy and the shims are stainless steel 0.8 mm thick. From the largest to the smallest spherical radius, the thickness of the rubber layers varies from 2 to 0.7 mm.

The number of shims was reduced from 16 to 13 and the total thickness of the rubber is increased by 13% and is the formulation *B* of the previous flexible bearing. The weight of this bearing is 2.8 kg.

The most highly stressed rubber layer in terms of service life is again the layer at the smallest spherical radius, but the combined stresses are reduced (see Fig. 9).

Stresses  $\tau_s$  and  $\tau_D$  and the pressure distribution are given at the same loads and displacements as for the preliminary flexible bearing (Fig. 10). With this new stress distribution, the theoretical increase in the service life is 21%; in fact, the actual service life of this new bearing is more than 2000 h, and

its stiffnesses remain within the requirements: compressive stiffness along the  $Oy$  axis is 105,000 N/m, and torsional stiffness about the  $Oy$  axis is 3.8 m·N/deg.

This new optimized flexible bearing meets all the requirements, service life included. The cost of this new bearing has also been reduced since there are fewer metal shims and the aluminum alloy attachments are cheaper to machine. This optimized flexible bearing was selected for production.

#### Hydroflex Bearing

For the layer where the combined stresses are the highest, the stresses  $\tau_s$  due to compressive forces along the  $Oy$  axis are a maximum near the inner diameter. These stresses can be reduced by eliminating the central hole and designing a bearing with continuous spherical layers. The combined stress is critical for the layer at the smallest spherical radius, but the critical point is now outside (Fig. 11).

The shear stresses  $\tau_s$  and  $\tau_D$  and the pressure distribution obtained at the same load and displacements as for the preliminary flexible bearing are shown in Fig. 12.

Compared with the previous optimized flexible bearing, the theoretical increase in service life is 168%. Unfortunately, such a design is very difficult to fabricate using the transfer molding process. To alleviate this manufacturing problem,

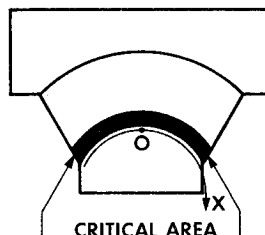


Fig. 11 Solid bearing.

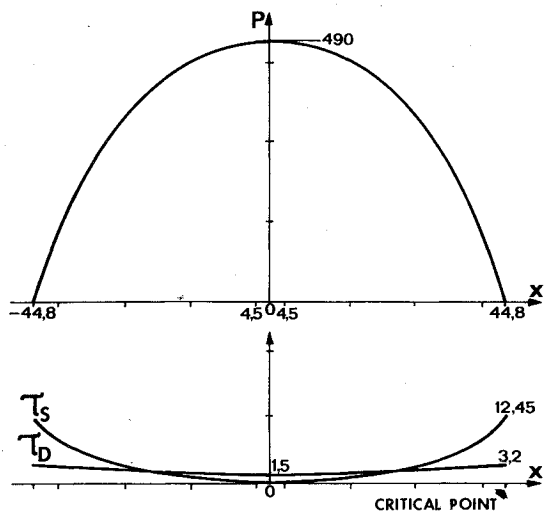


Fig. 12 Solid bearing—pressure and stress distribution.

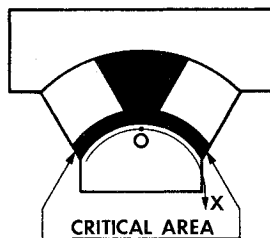


Fig. 13 Hydroflex bearing.

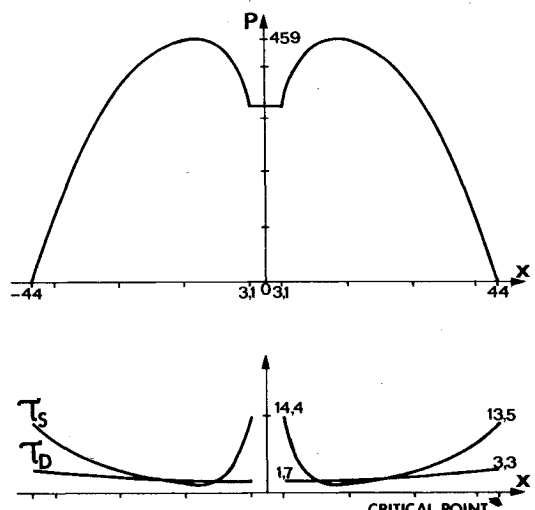


Fig. 14 Hydroflex bearing—pressure and stress distributions.

the central hole is filled with an incompressible liquid inert to the rubber, that is defined as the "hydroflex" technique (SEP patent pending). This liquid does not change the torsional stiffnesses about the  $Oy$  or  $Ox$  axes, but minimizes the stresses induced by a compressive force along the  $Oy$  axis as for the previous design without central hole.

As described previously, the bearing, a preliminary flexible bearing made with B rubber, has been modified to a hydroflex bearing. The central hole has been filled with a silicone oil. The new pressure and stress distributions in the layer where combined stresses are critical (smallest spherical radius) at the same conditions of load and displacement is as shown in Figs. 13 and 14.

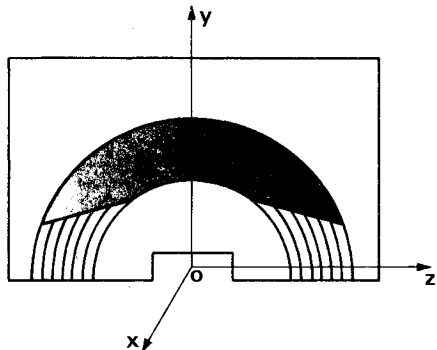


Fig. 15 High lateral stiffness hydroflex bearing.

The analysis of such a bearing has been performed according to the previously described method. The only difficulty is the definition of the pressure in the liquid, which is calculated using an iteration method based upon equating liquid pressure and rubber pressure at the boundary of the central hole.

The theoretical increase in service life is 152%. The critical area is outside. The torsional stiffness about the  $Oy$  axis is unchanged and the compressive stiffness along the same axis is increased. This hydroflex bearing has not been fatigue tested to failure. Hence, the actual service life is not known, but at 2000 h, no damage has been noticed, while the service life on the same bearing without liquid in the central hole was only 1500 h.

Another advantage of the hydroflex technique is that it is an easier design. There is less coupling between the various stiffnesses. For instance, it is now possible to design a bearing having a high stiffness along the  $Ox$  axis and be able to withstand a high load along the same axis (Fig. 15).

### Concluding Remarks

A spherical laminated elastomeric bearing for light helicopter rotor hub has been successfully developed and is now in production. The principal problem encountered has been that of service life, which is highly dependent upon geometry. The test results indicate that the hydroflex bearing will result in a significant increase in service life and is a simpler design.

### Acknowledgment

The author wishes to express his appreciation for the analysis contribution of F. Faye.

### References

- 1 Dutton, W. J., "Development of the H53 Elastomeric Rotor Head," 29th Annual National Forum of the American Helicopter Society, Washington, D.C., May 1973.
- 2 Mosinskis, V. S. and Schneider, E., "Design and Development of an Elastomeric Bearing Rotor Hub," 24th Annual National Forum Proceeding, May 1968.
- 3 Reddick, H., McCall, C. D., and Field, D. M., "Advanced Technology as Applied to the Design of the HLH Hub," 29th Annual National Forum of the American Helicopter Society, Washington, D.C., May 1973.
- 4 Gupta, B. P. and Finney, R. H., "Application of Finite Method to the Analysis of High Capacity Laminate Elastomeric (Incompressible) Parts," Society of Experimental Stress Analysis, May 1977.
- 5 Finney, R. H. and Bhagwati, B. P., "Design of Elastomeric Components by Using the Finite Element Technique," *Shock and Vibration Bulletin*, Sept. 1977.
- 6 Rijbicki, R. G., "The Sikorsky Elastomeric Rotor," American Helicopter Society, May 1979.